Journal of Achievements in Materials and Manufacturing Engineering

VOLUME 43
ISSUE 1
November
2010

Creep age forming: a short review of fundaments and applications

F.C. Ribeiro [a], E.P. Marinho [a], D.J. Inforzato [b], P.R. Costa [b], G.F. Batalha [c,*]

[a] Escola Politécnica da Universidade de São Paulo - Av. Prof. Mello Moraes, 2231 - Sao Paulo, Brazil

[b] Embraer – Empresa Brasileira de Aeronáutica S.A, Sao José dos Campos, Brazil

[c] Laboratory of Manufacturing Engineering – University of Sao Paulo Escola Politécnica – Av. Prof. Mello Moraes, 2231 – Cidade Universitária, CEP 05508900 – Sao Paulo, Brazil

* Corresponding author: E-mail address: gfbatalh@usp.br

Received 22.09.2010; published in revised form 01.11.2010

Analysis and modelling

ABSTRACT

Purpose: The aim is to review creep age forming theoretical fundaments as well as some of our experimental results.

Design/methodology/approach: The approach consists of a brief review from basic theoretical concepts of creep and ageing processesincluding a description of anumeric closed form technique to predicting springback in creep age forming. Finally, a work flow to develop a creep age forming process and its respective experimental implementationare shown.

Findings: The analytical model and workflow enabled an excellent result of springback predicted value (less than 1%).

Research limitations/implications: The experiments only tested simple parts. An improved model is necessary for more complex parts.

Practical implications: This work permits to study the creep age forming viability of a given process planning.

Originality/value: This review summarizes the main concepts of the creep age forming process and illustrates them by the application of an analytic and numerical modelling performed as a didactic experiment.

Keywords: Creep age forming; Age forming; Creep forming; Springback

Reference to this paper should be given in the following way:

F.C. Ribeiro, E.P. Marinho, D.J. Inforzato, P.R. Costa, G.F. Batalha, Creep age forming: a short review of fundaments and applications, Journal of Achievements in Materials and Manufacturing Engineering 43/1 (2010) 353-361.

1. Introduction

Creep Age forming (CAF), also known as Age forming or Creep forming, is a process in which a part, usually an aluminium machined plate, is forming by creep on a tool at the same time that an ageing precipitation heat treatment is conducted [1]. CAF is generally carried out within an autoclave. Vacuum is formed between the plate and the tool through of a vacuum bags assembly. When the autoclave pressure is raised, stage 1, the part is moulded on the tool and, if necessary, an extra pressure can be imposed by mechanical equipment. For the second stage, the residence time and temperature used in autoclaves are optimized for the ageing heat treatment [2]. Therefore, the part reaches the best mechanical performance, hardening and strength. Later, creep is interrupted and the stress relaxation is not the maximum possible. Thus, after the part is removed from tooling, stage 3, the plate undergoes about 70% springback. Figure 1 illustrates the CAF process. This process is relatively recent. CAF started to be studied in the 1980s by Textron, aiming large aluminium panels

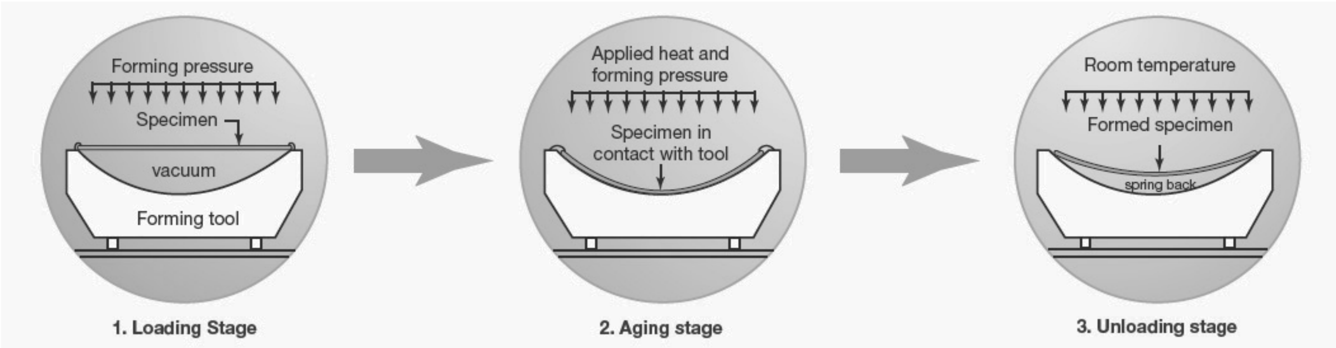

Fig. 1. Creep age forming process stages [3]

of about 15 m, to attain airfoil sections and complex curvatures. Textron developed a closed equation for beam and cylindrical CAF mold as well. The first aircraft to receive CAF parts was the USAF. B-1B Long Range Combat Aircraft. Both the upper and lower wing skins were manufactured using CAF. The Gulfstream G-IV project marks the first time a double curvature wing panel was made using CAF techniques. CAF was applied in Airbus 330 and 340 imparting twist and curvature to extruded stringers [4]. In the UK, Qinetq developed the wings manufacturing process for Airbus 380. Both skins and strings were made using the CAF process [2].

More recently, a consortium was formed by Alcan as an aluminium supplier, the University of Manchester focused on of the metallurgical interactions in the age forming process, Dassault Aviation representing executive aviation, Airbus representing commercial aviation, Sabca concerned with space structures for the Ariane program and Alenia, interested in studying new methods for fuselage. Figure 2 shows a panel jointly developed by this CAF consortium [3].

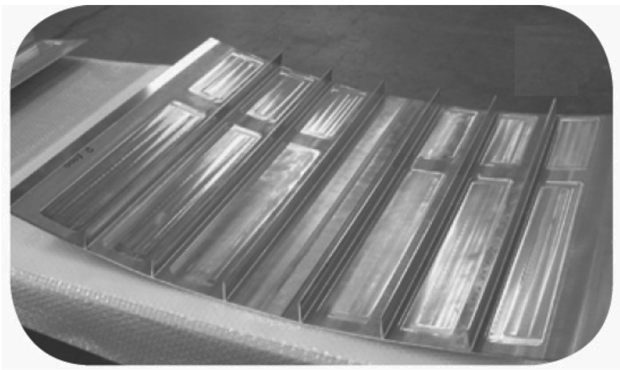

Fig. 2. Creep Age forming demonstrator. Alenia [3]

One of the desires of the aviation industry is to manufacture structures with higher stiffness and strength, and low weight. In the context, to use creep age forming implies that the manufacture of the wing, skins and stringers, can be made entirely from the machining of a single aluminium block, see Figure 3. Therefore, at the same time that this desire becomes possible, there is no need to have built-up steps with rivets or welding, therefore decreasing the manufacturing cost. Figure 4 shows costs comparison. Moreover, unlike all concurrent process, peen forming, stretching and roll forming, CAF is not carried out in plastic regime and, therefore, the residual stress level is significantly lower [4].

Fig. 3. Integral stiffened wing skin [6]

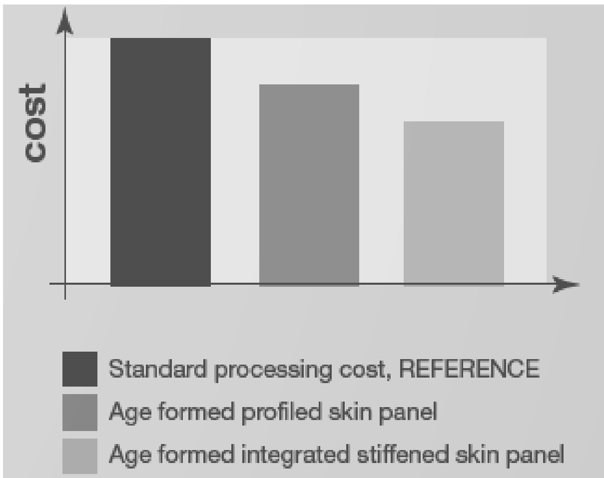

Fig. 4. Cost comparison between forming processes [3]

Conventional forming methods such as roll forming, stretch forming and peen forming are based on plastic deformation and generate a high residual stress that can cause problems when the material is loaded dynamically. Moreover, the conformation of parts with sharp differences in thickness requires special manufacturing equipment and the process may not even be viable. Figure 5 compares the residual stress between some forming methods.

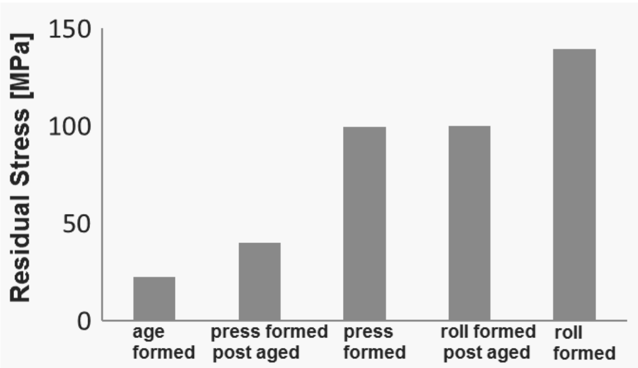

Fig. 5. Tensile residual stress measurements of aluminium alloy 7075 formed to the same radius of curvature adapted from [6]

Among creep age forming drawbacks, there is the difficulty in predicting the springback, how to compensate it in the tool shape design and restrictions for heat treating the material [1].

Around the world, some groups have studied creep age forming. In the United Kingdom, the University of Manchester participated in the Ageform project; the University of Birmingham and the Imperial College developed a closed form to predict the springback and residual stress for CAF [7-10]. This model will be the modeling focus of this paper. In France, some groups carried out some studies using creep models to predict the curvature of an integrally stiffened structure [11-12]. In China, researchers of Beijing University of Aeronautics and Astronautics carried out some finite element analysis using creep models as well [13].

Our aim is to review the basic concept of the CAF process. In order to do it, the text is divided into three parts. First, the theoretical basis of creep and ageing phenomena is presented and a creep age forming model is explained. Later, a workflow to carry out creep age forming is shown. Finally, experimental results using analytical springback prediction equation of cylindrical plate forming is described.

2. Creep age forming modelling

Exposing some process features, this item describes the creep and ageing processes phenomenological and mathematically. First, each process is studied separately and then a coupling between creep and ageing is searched.

2.1. Ageing hardening

Aluminium alloys that contain a combination of elements such as Cu, Mg, Zn, Sc, are involved in the more noble applications in the industry. The addiction of these elements allows developing high performance alloys through heat treatments.

These atoms, when added to the aluminium matrix during ageing, progressively form solute segregation, further resulting in precipitation. To conduct the ageing process of a workpiece, the first step is to warm it to the point that all solute is solubilized. Note that this temperature must be less than the $\alpha + L$ line limit of the phase diagram, Figure 6. After a rapid cooling (quench), a supersaturated microstructure of solute and vacancies in aluminium matrix is obtained. Therefore, the solid solution is thermodynamically unstable.

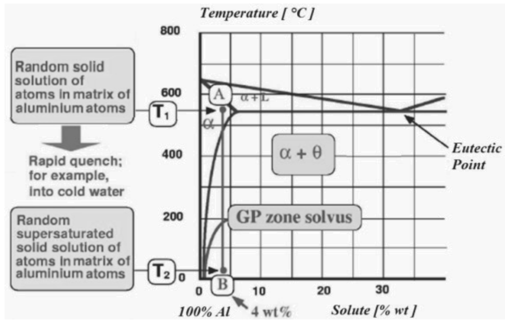

Fig. 6. Aging, solving and precipitation hardening at heat treatable aluminium alloys. Adapted from [4]

In order to reduce the system energy, diffusion of atoms and vacancies occurs. Hence, as the atoms gather in clusters, they precipitate and hinder the sliding between atomic planes and the aluminium matrix. This microstructural phenomenon reflects macroscopically in better mechanical properties such as strength and hardness. However, this behaviour has a hardness peak. When the grain size is zero, there is any precipitate. After certain ageing time, coarsening occurs and the microstructure reaches a state at which the best combination between grain size and number of clusters occurs and hinders dislocation movements. Beyond this time, the cluster coarsening makes the number of clusters be small and the dislocation movement becomes easier. Analogously, vacancies come together and form large voids within the material. Due to both phenomena, the alloy hardness and strength decreases [14]. In the ageing hardening modelling presented by Shercliff & Ashby, [15-16], there is a need to study the microestrutural evolution kinetic together with the dislocation behaviour to predict mechanical properties. Internal state variables are used to mathematically describe the microstructure. Differential concerning the time of these variables describes the mechanical properties in relation to process evolution. In a simplified form, aluminium microstructure can be described by two states variables: the volume fraction of precipitate, f, and the average particle radius, r. Hence, there are two state equations (1, 2).

$$\frac{\partial r}{\partial t} = g_1(r, f, T, \ldots) \qquad (1)$$

$$\frac{\partial f}{\partial t} = g_2(r, f, T, \ldots) \tag{2}$$

The autoclave temperature in CAF is constant. Hence, the modelling focus will be on isothermal ageing. In this case, it is possible to consider a constant value for f equal to the equilibrium at a given temperature. Therefore, equation (2) is zero and the problem can be described just by state variable radius. In the isothermal hardening model, factors that influence the aluminium alloy yield stress, the f value, the temperature dependence, the precipitated coarsening and the contribution of solute depletion in material matrix must be included. Coarsening is described by the average radium growth as a function of time. It is assumed that only a unique type of precipitate dominates the mechanical behaviour during the ageing process. Strengthening in material resistance due to the volume fraction of precipitate for a given radius r depends on the kind of interaction between the dislocations. For precipitate under shearing, the increment in yield stress is given by

$$\Delta\sigma_{ps} = C_1 f^{0.5} r^{0.5} \tag{3}$$

while that for contoured precipitated

$$\Delta\sigma_{pb} = C_2 f^{0.5} r^{-1} \tag{4}$$

where C_1 and C_2 are constant of materials.

Precipitate coarsening to a fixed volume fraction can be described as function of r defined by

$$r^3 = r_0^3 + C_3\left[\frac{t}{T}\left(e^{-\frac{Q}{RT}}\right)\right] \tag{5}$$

thus, the precipitate coarsening can be defined as:

$$P = \left[\frac{t}{T}\left(e^{-\frac{Q}{RT}}\right)\right], \tag{6}$$

to represent the precipitation hardening kinetics. Examination of ageing curve data reveals that the value of P required to reach the peak over a wide range of temperature is often roughly constant. Hence, the value Pp is used to normalize the kinetic strength (noting that P/Pp = 1 at the peak). Over most of the ageing curve, the initial radius r_0 << r, hence equation (5) can be re-write as

$$r = C_4\left(\frac{P}{P_p}\right)^{1/3}. \tag{7}$$

Therefore, equations (2) and (3) become

$$\Delta\sigma_{ps} = 2S_0\left(\frac{P}{P_p}\right)^{1/6} \tag{8}$$

and

$$\Delta\sigma_{pb} = 2S_0\left(\frac{P}{P_p}\right)^{-1/3} \tag{9}$$

S_0 Consists in only one material property that is a combination of C_1, C_2, C_3 and C_4 constants.

The strength increment caused by precipitation due to these two mechanisms will be approximated by harmonic mean. Hence, equation (8) describes the yield stress rise.

$$\Delta\sigma_p = \left[\frac{1}{\Delta\sigma_{ps}} + \frac{1}{\Delta\sigma_{pb}}\right]^{-1} = 2\,\frac{S_0\left(\frac{P}{P_p}\right)^{1/6}}{1+\left(\frac{P}{P_p}\right)^{1/2}} \tag{10}$$

From equation (8), it is possible to conclude that S_0 is the maximum increment in material yield stress and $\Delta\sigma_p/S_0$ is dimensionless. Consideration of a *solvus* limit in the phase diagram (4) leads to an expression for S_0 temperature dependence:

$$S_0^{\,2} = S_{0\,max}^{\,2}\left[1-\exp\left[-\frac{Q_s}{R}\left(\frac{1}{T}-\frac{1}{T_s}\right)\right]\right] \tag{11}$$

Where, S_{0max} is the value that would be found if all solute precipitated, Q_s is the solute enthalpy and T_s is temperature of *solvus* boundary at the phase diagram. Thus, five material properties are needed in order to use this model: P_p, Q, $S_{0\,max}$, Q_s and T_s.

The first three properties can be obtained by performing a hardness test. The hardness graph shows peak time and P_p. After measuring, $\Delta\sigma_p$, $S_{0\,max}$ is found, as well. Extracting the natural logarithm in (6), Q is obtained. Values Q_s and T_s are found in $S_s$vesus temperature graphic that is shown in Figure 7. These steps are illustrated in Figure 5. Some model results are shown in Figure 8.

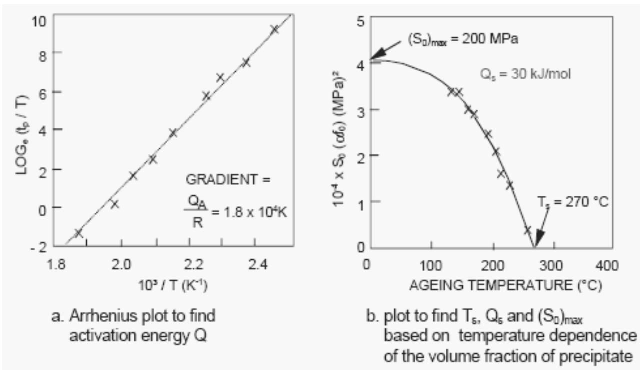

Fig. 7. Calibration of the isothermal ageing model [14]

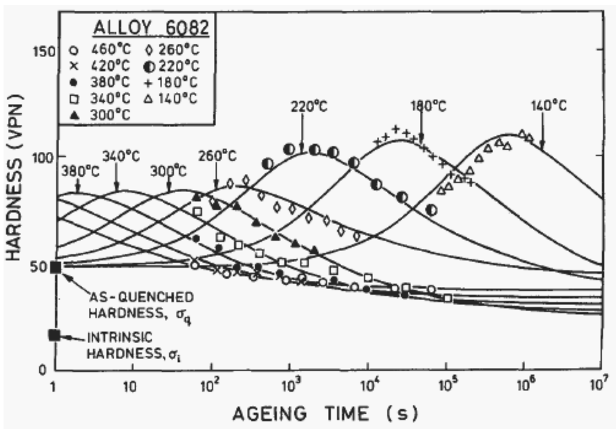

Fig. 8. Comparison between measured and predicted data [15]

2.2. Creep deformation and stress relaxation

Creep is an inelastic deformation that occurs continuously and slowly over time when structure is loaded to a stress below yield stress under a temperature higher than about 30% of the material melting temperature [17]. Therefore, mathematically, the creep strain can be expressed by

$$\varepsilon = f(\sigma, t, T) \tag{12}$$

In Figure 9, typical curves of a creep test with stress and fixed temperature are shown. The graphic shows three distinct behaviours commonly called creep stages. In the First stage, or transient stage, there is a decrease in the strain rate. In the second stage, or steady-state stage, the strain hardening effect balances with the structural recovery and the strain rate becomes null. The third state drives the workpiece to fracture and the strain rate increases over time. At this stage, different damage phenomena occur, such as nucleation, cavities growth, necking and crack propagation. These mechanisms decrease the cross-section area and increase the stress onto the material ultimate stress [18].

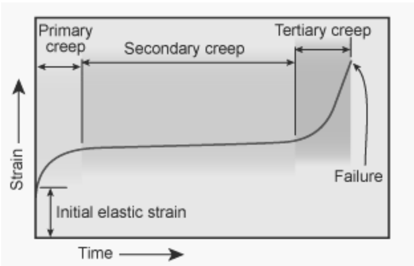

Fig. 9. Typical creep test curve

After a description of creep by a state-variable approach and to know the creep mechanisms, it is also important to understand the CAF equation also involving damage variables.

Creep by dislocations occurs when a crystalline material is deformed plastically. The required stress to cause yielding is that needed to make the dislocations overcome the intrinsic lattice resistance and overcome the obstructing effect of obstacles. If the temperature increases, the diffusion, obeying Fick`s law, increases as well and helps the atoms movement that unlocks dislocations. These, under applied stress, lead to dislocation creep. This mechanism outlines the climb and glide movements. Both mark the dislocation movements. First, the dislocation movement itself in the stress direction, in other words, planes slide up to the obstacle. This configures the glide phenomenon. The movement to contour the precipitated, climb, occurs by diffusion, but is governed by part stress that accounts for the climb force [19].

As the relaxation of initial stress occurs, the dislocation creep rate decreases rapidly. However, as there is still energy to cause diffusion, this becomes dominant and is directed by the remaining low stress. Now, the creep rate stays proportional to the diffusion constant, normal stress and inversely proportional to grain size, d, square. This occurs because the higher grain implies more time for the atom to reach the contour.

To understand the relaxation phenomenon, suppose that a plate is bent on a tool and the stress is lower than the yield stress. The total stress will be a constant value and initially equal to the elastic strain. If the part is warmed, creep strain begins and equation (13) must be obeyed.

$$\varepsilon^{total} = \varepsilon^{elastic} + \varepsilon^{creep} \tag{13}$$

ε^{creep} is always positive and grows monotonically with time, the elastic deformation has to decrease with time and, therefore, stress decreases. If isothermal creep is considered, the elastic strain graphic represented by $\sigma/_E$ assumes the shape illustrated in Figure 10.

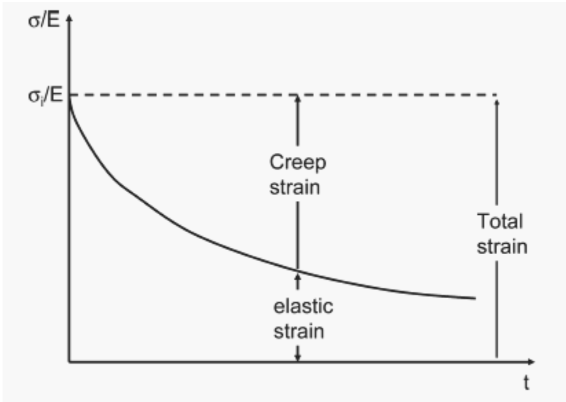

Fig. 10. Stress relaxation [19]

2.3. A coupled creep age forming model

After a preview explanation of creep and ageing phenomena separately, now the coupling of both phenomena will be dealt with [20-21].

The precipitated presence disturbs the dislocation movement, and therefore decreases the creep rate. On the other hand, the dislocation movement caused by the stress imposed creates shear in the precipitated; therefore, the creep contributes to part hardening. This coupling is described by the classical plasticity theory by equation (14).

$$\varepsilon^{total} = \varepsilon^{elastic} + \varepsilon^{creep} - \varepsilon^{ageing} \tag{14}$$

where $\varepsilon^{ageing} = {}^{\Delta\sigma_P}/_E$. However, to use this approach would be a hard task. Thus, the inelastic theory is applied. Now, equation (15) becomes:

$$\varepsilon^{total} = \varepsilon^{elastic} + \int_0^t \dot{\varepsilon}^{inelastic}\, d\tau \tag{15}$$

Where the kinetics law, or flux law, is written formally as

$$\dot{\varepsilon}^{inelastic} = \dot{\varepsilon}^{inelastic}(\sigma, T, \mu_k, \ldots) \tag{16}$$

and μ_k are state variables that are used as macroscopic measures of microstructure features. The evolution equations to update the current values of the state variables are formally given as

$$\dot{\mu}_k = \dot{\mu}_k\left(\dot{\varepsilon}^{inelastic}, \sigma, T, \mu_i, \ldots\right) \quad (17)$$

The next step is to identify the state variables for CAF problems. Kowalewski [22] suggests using the dislocation hardening, H, to accompany the creep event and using the precipitated radius, r, to represent the ageing event. With these two state variables, it is possible to describe the first and the second creep states occurring under ageing effects. The third stage is not interesting for CAF because it introduces damage to the workpiece.

As output data, the model permits to get a graphic of inelastic deformation *versus* time and, with this, it is possible to obtain the part springback after the forming process. The residual stress and the yield stress can be predicted as well.

The springback is defined as the relative diminution of deflection at the center of the plate before and after the tool is retrieved [7]:

$$\text{springback}\ (\%) = 100\%\left(1 - \frac{\delta^f}{\delta^o}\right) \quad (18)$$

The choice of the springback definition can be justified by its widespread use in the literature. Other definitions exist, including curvature. But this form has a simple physical interpretation.

The following equation set (19-25), proposed by Jeunechamps [7], represent the model for plate forming with double curvature by creep age forming process.

$$\dot{\varepsilon}^{inelastic} = A.\sinh\left\{B[(\sigma_e - \sigma_A)(1-H)]\left(\frac{C_{ss}}{\sigma_{ss}}\right)^n\right\} \quad (19)$$

$$\dot{H} = \frac{h_c}{\sigma_e^{0.1}}\left(1 - \frac{H}{H^*}\right) \quad (20)$$

$$\dot{r} = C_0(Q-r)^{m_0}\left(1 + \left|\frac{\dot{\varepsilon}^{inelastic}}{\gamma}\right|^{m_1}\right) \quad (21)$$

$$\sigma_A = C_A r^{m_2} \quad (22)$$

$$\sigma_{SS} = C_{SS}(1+r)^{-m_2} \quad (23)$$

$$\sigma_Y = \sigma_{SS} + \sigma_A \quad (24)$$

The constants A, B, h_c, H^*, n, Q, C_0, γ, C_A, C_{SS}, m_0, m_1, m_2 are material constants, which are determined experimentally.

Equation (19) describes the evolution of the inelastic strain that represents the creep age strain. The adaptation of the Miller equation for creep is employed. The effective stress due to bending of the plate over the tool is subtracted from the stress increment given by ageing. To describe the first and second stages, state variable H is included. Note that if $H < H^*$, by eq. (21), the derivative of eq. (20) decreases as an expected behaviour for the first stage and becomes null for $H > H^*$. Value H^* marks the saturation value at the end of the primary period. Physically, parameter H represents the micro indentation hardness dimensionless variation and this variable runs as a time event measure. Microscopically, the dislocations slide until they find an obstacle while $H < H^*$ and with this dislocation, hardening happens. When H reaches H^*, dislocation creep rate drops because almost all dislocations are stopped near obstacles. Then, diffusional creep turns predominant to carry out glide and climb movements. Finally, factor $\left(\frac{C_{ss}}{\sigma_{ss}}\right)^n$ is used to consider the softening of the matrix material due to coarsening. This factor favors dislocation movement caused by creep.

Equation (20) is the equation that describes the state variable H. The other state variable, modeled in eq. (21), describes the evolution of the precipitated radius during the isothermal ageing mechanism. Eq. (6) is not used because it does not consider the creep phenomenon. Eq. (22) includes the creep strain rate to describe the dynamic ageing behavior given by factor $\left(1 + \left|\frac{\dot{\varepsilon}^{inelastic}}{\gamma}\right|^{m_1}\right)$. As the creep deformation (or dislocation density) increases, the age-hardening effect is favored. The term Q, a material constant for a given alloy, is used to represent the saturation limit for depletion of the zinc solute atom. The power term, m_0, gives flexibility to the equation as different alloys behave differently. Generally, $m_0 = 1/3$ because of exponent 3 in equation (5).

Equations (22), (23) and (24) were presented in the ageing hardening section. They describe the ageing contribution to the increment of the yield stress given by σ_Y. Parameter C_A is the material property that describes the interaction between dislocations and precipitated while the coarsening occurs at the volume fraction of precipitate constant. Eq. (24) shows that, with the appearance of precipitate, the concentration of atomic solute decreases and, hence, σ_{SS} decreases as well.

3. Creep age forming work flow

As stated before, creep age forming has two main restrictions. First, the alloy ageing time should be long enough to make it logistically possible to solubilize the part in a heat treatment and to assemble it on the tool. For example, 2XXX alloys is not creep age formable because they ageing time is too fast [2]. Second, the part stress after pressure loading on the tool should be lower than the yield stress. Stress higher than yield stress does not allow the creep deformation to occur because there is plastic deformation. As before mentioned, one of CAF advantages over peen forming is that it does not generate plastic deformation and, therefore, CAF does not introduce damage or high residual stress in the part.

Given that the alloy is known, CAF assessment consists in determining the stress of the part in the loading step. This means that it is enough to utilize an elastic material model for the initial stress prediction. For a single or double curvature sheet, there are some analytical models in the elasticity theory, but if the part is more complex, for example, upper wing jet with reinforced welding, there is the need to carry out a finite element analysis to simulate contact between part and tool.

The next step is to determine creep age forming time, in the other words, how long the part will stay within the autoclave. This variable is chosen to optimize mechanical properties. As these are given by the ageing process, the springback is calculated supposing ageing at the optimal point.

For each alloy, experiments have to be carried out to determine the CAF time or ageing properties.

Hardness increases monotonically up to a peak and decreases monotonically, as well. Hence, it is necessary to control the material ageing state before the creep age forming process starts. Imagine that a part at peak hardness is put in the autoclave for CAF. After 20 hours, material properties would be completely improper.

To prepare the material for CAF, it is necessary to solubilize the material to obtain a supersaturated microstructure of solute and vacancies. The precipitated radius is zero in this state. To facilitate the plate machining process, if any, pre-ageing is realized carried out before CAF.

With ageing parameters obtained, creep parameters have to be found. The creep test is conducted using a tensile specimen to which a constant stress is applied, often by the simple method of suspending weights from it. Surrounding the specimen is a thermostatically controlled furnace, the temperature being controlled by a thermocouple welded to the gauge length of the specimen. The extension of the specimen is measured by a very sensitive extensometer since the actual amount of deformation before failure may be only two or three per cent. The results of the test are then plotted in a graphic of strain versus time to give a curve similar to that illustrated in Figure 3.

All parameters obtained, the next step is to implement the CAF model in a finite elements analysis program. Due to the fact that creep age form is recent, the main FEA programs do not have creep age forming routines ready to use. However, these programs have user subroutines for creep that allows writing a FORTRAN code.

The last step is to find the tool surface that compensates springback effects and, after CAF, to obtain a part similar to the CAD geometry. A CAF tool is shown in Figure 11.

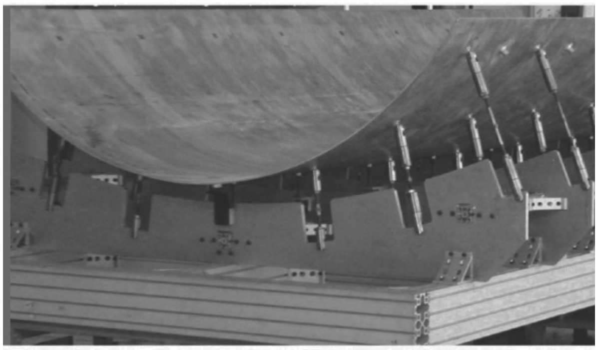

Fig. 11. Fuselage panel forming tool

4. Results

For the experimental tests, the step sequence suggested by the workflow presented was carried out for a simple case. A 12 mm x 100 mm x 300 mm AA7475 aluminium alloy plate was age formed on a cylindrical tool to final part radius equal to 12 m. The springback was predicted using the analytical form and compared with experimentally measured springback.

As stated before, the first step is to assess the stress level after the pressure loading. A finite element analysis was implemented in the MARC software to simulate the part stress due to contact between part and tool caused by a 6.9 bar pressure. Figure 12 shows the stress map.

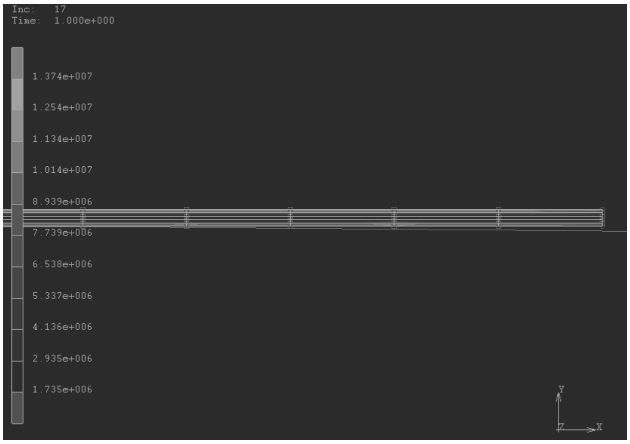

Fig. 12. Von Misses stress (N/m2) in a sheet after CAF loading

The creep age forming time and temperature was obtained in the military specification MIL-H-6088. The ageing time was considered to reach temper T7651. To avoid the solubilisation step, the material initial temper was W (Table 1).

Table 1.
Experimental CAF Process variables

Process variable	*Value*
Temperature	163C
Ageing time	24 hours
Pressure	6.9 bar

The creep model used to predict the springback is analytical and is valid for cylindrical mould [23].

$$\text{springback}\ (\%) = 100\% \left(\frac{\sigma_f}{\sigma_i}\right) \qquad (25)$$

where σ_f must be known experimentally as a result of a relaxation test, and σ_i is related to the tool curvature. The tool radius equal to 3750 mm was obtained by equation (26) and then the tooling was developed and is shown in Figure 13.

Fig. 13. Tooling manufactured for the CAF experiment [2]

The test sample was prepared in the tooling through vacuum bag techniques similar to those is used for compound materials cure. See Figure 14.

Fig. 14. Vacuum bag technique applied in CAF test [2]

After the creep age forming was concluded, the part underwent a measurement stage in a CNC coordinate measure machine and the experimental springback was measured according to equation (18) in three different sections. The comparison between the predicted and the experimentally obtained springback is shown in Table 2.

Table 2.
Springback comparison for CAF test and modelling

	SECTION 1	*SECTION 2*	*SECTION 3*
MEASURED SPRINGBACK (mm)	87.30	86.91	82.02
PREDICTED SPRINGBACK (mm)	86.32	86.32	86.32
VARIATION (mm)	-0.98	-0.61	0.30
VARIATION (%)	-1.1%	-0.68	0.37

5. Conclusions

The method presented allows a rapid assessment of the CAF process suitability.

The accuracy obtained experimentally validates the analytical model. Although this analytical model is not sufficient for the manufacture of parts that have complex geometries, such as reinforced wing skins, it already allows the manufacture of simple parts and subsequent built-up. For example, it is possible to bend a plate and the beams separately and then perform the assembly by welding or riveting.

Acknowledgements

The authors thank CAPES, CNPq and EMBRAER for the grants and financial resources that are supporting the framework of this project.

References

[1] F.C. Ribeiro, P.F. Marinho, D.J. Inforzato, G.F. Batalha, Creep Age Forming Modeling, Proceedings of the 30th Conferência Nacional de Conformação de Chapas, Porto Alegre, Rio Grande do Sul, Brazil, 2010 (in Portuguese).

[2] P.F Costa, C. Moura Neto, D.J. Inforzato, Assessment of Al7475 plates springback submitted by creep age forming process, Proceedings of the 65th Congress da – Associação Brasileira de Metalurgia, Materiais e Mineração, Rio de Janeiro, 2010 (in Portuguese).

[3] Age forming project brochure, Available at 16 October 2010 on http://www.scribd.com/doc/37472248/AgeForm.

[4] M.C. Holman, Autoclave age forming large aluminum aircraft panels, Journal of Mechanical Work Technology 20 (1989) 477-488.

[5] K. Watcham, Airbus A380 takes creep age-forming to new heights, Materials World 12/2 (2004) 10-11.

[6] P.P. Jeunechamps, K.C. Ho, J. Lin, J.P. Ponthot, T.A. Dean, A closed form technique to predict springback in creep age-forming, International Journal of Mechanical Sciences 48 (2006) 621-629.

[7] K.C. Ho, J. Lin, T.A. Dean, Modeling of springback in creep forming thick aluminum sheets, International Journal of Plasticity 20/4-5 (2003) 733-751.

[8] K.C. Ho, J. Lin, T.A. Dean, Constitutive modeling of primary creep for age forming an aluminum alloy, Proceedings of the International Conference "Advances in Materials and Processing Technologies" AMPT2003, Dublin, 2003, 615-618.

[9] A. Deschamps, Modeling of microstructure evolution and mechanical properties in age-hardening aluminum alloys, Proceedings of the European Congress "Advanced Materials and Processes" EUROMAT 99, Germany, 1999, v. 3, 121-132.

[10] B. Escoffier, Y. Chastel, A. Pineau, G. Sola, G. Surdon, Physical and mechanical modeling of ageforming in 7050 Al Alloy, Proceedings of the 22nd 3AF Colloquium, Material For Aerospace Applications, 2007.

[11] G. Sola, G. Surdon, Y. Chastel, A. Pineau, Développement d'un modèle rhéologique de fluagerelaxation de l'aluminium 7050 pour le formage au revenue de panneaux de voilure, Proceednigs of the 9th Colloque National en Calcul des Structures, Giens, France, 2009 (in French).

[12] H. Lina, W. Mina, C. Cailoub, J. Xiushengb, FEM Analysis of Spring-backs in Age Forming of Aluminum Alloy Plates, Chinese Journal of Aeronautics 20/6 (2007) 564-569.

[13] M.H. Jacobis, Process Precipitation Hardening, TALAT Lecture 1204, TALAT.

[14] Ø. Grong, Process Modeling Applied to Age Hardening Aluminum Alloys, TALAT Lecture 1601, TALAT.

[15] H.R. Shercliff, M.F. Ashby, A process model for age hardening of aluminium alloys-II, Acta Metallurgica et Materialia 38 (1990) 1789.

[16] Y.M. Haddad, Viscoelasticity of Engineering Materials, First Edition, Chapman & Hall, London, 1995.

[17] M.F. Ashby, D.R. Jones, Engineering Materials, First Edition, Butterworth-Heinemann, UK, 1980.

[18] S. Spigarellin, Creep of aluminum and aluminum alloys, TALAT Lecture 1253, TALAT.

[19] D.C. Stouffer, Inelastic Deformation of Metals, First Edition, John Wiley, EUA, 1996.
[20] D.S. Chan, U.S. Lindholm, S.R. Bodner, K.P.A. Walker, Survey in unified constitutive theories, Proceedings of the 2nd Symposium NASA-LEWIS Non-linear Constitutive Relationship High Temp. Appl., Cleveland, USA, NASA Conference Publications 2369, 1985.
[21] Z.L. Kowalewski, D.R. Hayhurst, B.F. Dyson, Mechanism-based creep constitutive equations for an aluminum alloy, Journal of Strain Analysis 29 (1994) 309-316.
[22] M. Sallah, J. Peddieson Jr., S. Foroudastan, A mathematical model of autoclave age forming, Material Processing Technology 28 (1991) 211-219.